Delay-Doppler Waveform Analysis and Synthesis in MIMO Integrated Sensing and Communications

Husheng Li

GLOBECOM 2024 - 2024 IEEE Global Communications Conference | 979-8-3503-5125-5/24/$31.00 ©2024 IEEE | DOI: 10.1109/GLOBECOM52923.2024.10901448

***Abstract*—The technique of Integrated Sensing and Communications (ISAC) is expected to be one of the six pillars of 6G wireless communication systems. It integrates communications and sensing in the same waveform, thus substantially reducing the consumption of bandwidth. When multiple antennas are used for both ISAC transceiver and communication receiver, new techniques of waveform synthesis are needed for the multiple-input-multiple-output (MIMO) ISAC. In this paper, a generalized ambiguity function (AF) is proposed for the MIMO ISAC, based on which the trade-off between communications and sensing in MIMO ISAC is quantified. Numerical simulations are used to demonstrate the validity of the proposed generalized AF and quantify the fundamental trade-off in MIMO ISAC.**

***Keywords*—** Integrated Sensing and Communications; MIMO; Doppler shift; ranging; ambiguity function

I. Introduction

Recent years witness the resurrection of Integrated Sensing and Communications (ISAC), due to the expected development in the 6G wireless communication standards, and the promising applications in various cyber physical systems (CPSs) such as vehicular ad hoc networks (VANETs) or urban air mobility (UAM). In ISAC, the same waveform can carry messages for communications in the forward propagation and fetch the information of significant reflectors in the backward propagation, such that both bandwidth and power are efficiently utilized.

The main challenge of ISAC is how to integrate both functions of data communications and radar sensing in the same waveform. To this end, we need to understand and quantify the requirement of both functions on the waveform. For example, radar sensing desires non-stationary waveforms (such as the frequency modulation continuous wave (FMCW) in which the carrier frequency changes linearly with time) for a better timing information, while communications prefer stationary carriers (such as sinusoidal function at the carrier frequency).

There have been significantly many studies on the ISAC design for single-antenna systems, proposing many design criteria [1]–[3]. However, they cannot be straightforwardly extended to the multiple-input-multiple-output (MIMO) case, although MIMO techniques are critical for both communications [4] and radar [5]. Therefore, there is a pressing demand to study the waveform synthesis in MIMO ISAC. Although there have been significant studies on MIMO ISAC, which will be detailed in subsequent section, they are more focused on beamforming for multiplexing the signals of communications and sensing, instead of exploiting the diversity incurred by the multiple antennas. Moreover, most existing studies on MIMO ISAC omitted the consideration of Doppler shift and velocity estimation.

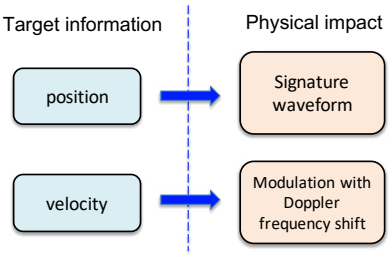

Fig. 1: Mapping of target information to physical signal features.

For the sensing in MIMO ISAC, in the near-field case, the relationship between the radar target (as the significant reflector) information and the physical feature of echoed signal is given as follows, as illustrated in Fig. 1:

- Position: The position of target is characterized by the corresponding signature vector of received signals at different antennas, since the traveling distance determines the phase of received signal. They also cause time delay for the communication receiver.
- Velocity: The motion of the target incurs a Doppler shift in the frequency, and thus a modulation by an oscillation. It causes a frequency offset at the communication receiver.

We will first generalize the ambiguity function (AF) [6] in traditional radar theory to the MIMO case, which incorporates the impact of communications, and then quantify the performance trade-off between communications and sensing in MIMO ISAC.

The remainder of the paper is organized as follows. The related works are briefly introduced in Section II. The system model is explained in Section III, based on which the gen-

H. Li is with the School of Aeronautics and Astronautics, and the Elmore Family School of Electrical and Computer Engineering, Purdue University, USA (email: husheng@purdue.edu). This work was supported by the National Science Foundation under grants 2052780, 2135286, 2109295 and 2128455.

eralized AF is defined in Section IV and the fundamental trade-off between communications and sensing in MIMO ISAC, is discussed in Section V, respectively. The numerical results and conclusions are given in Sections VI and VII, respectively.

II. Related Works

Excellent comprehensive surveys on ISAC can be found in [7]–[9]. For MIMO ISAC, the spatial separation of communications and sensing via beamforming [8]–[10] is demonstrated to achieve higher spectral efficiency than time/frequency separation. A comprehensive survey on the important results of MIMO broadcast communications can be found in [11]. A few studies on the waveform design of ISAC can be found in [12]–[16]. However, there have not been studies on the trade-off between communication channel capacity, positioning and Doppler velocity estimation in the context of MIMO ISAC.

III. System Model

In this section, we introduce the system model of MIMO ISAC, particularly the impacts of position and Doppler shift of the sensed target.

A. System Configuration

We assume that the ISAC transceiver has N_t transmit antennas and N_r receive antennas. The communication receiver has N_c antennas. We assume K significant reflectors as radar targets. The local parameters of reflector k are denoted by $\theta_i(t) = (\mathbf{q}_k(t), \mathbf{v}_k(t))$, where $\mathbf{q}$ and $\mathbf{v}$ denote the time-varying position and velocity of the reflector, respectively. For simplicity, we consider the planar case, such that $\mathbf{q}$ and $\mathbf{v}$ are both 2-dimensional. The communication receiver is assumed to be stationary, whose position is denoted by $\mathbf{q}_0$. The origin of the reference frame is set at the center of the ISAC transmitter. The total bandwidth used by the ISAC signal is denoted by W, while the available transmit power is P_t.

B. Single Carrier: Time-domain Signaling

We first consider single-carrier signals with carrier frequency f_c, whose design is in the time domain on the signaling.

1) Continuous-time Signals: We assume that the transmitted signal at the N_t transmit antennas is given by

$$\mathbf{s}_t(t) = e^{j\omega_c t}\mathbf{W}\mathbf{s}(t), \tag{1}$$

where $\mathbf{s}(t) = (s_1(t), ..., s_{N_t}(t))$ is the N_t-dimensional vector of the baseband (but not necessarily narrowband) signal, $\mathbf{W} = (w_1, ..., w_{N_t})$ is the diagonal matrix consisting of the complex weights at different transmit antennas, and $\omega_c = 2\pi f_c$ is the carrier angular frequency. All the signals $\{s_n(t)\}_{n=1,...,N_t}$ are of bandwidth W. The time duration of the waveform is denoted by T_p, where the subscript p means radar pulse. For simplicity, we assume that $E[|s_n(t)|^2] = 1$ and $\sum_{n=1}^{N_t} |w_n|^2 = P_t$. Note that $\mathbf{s}(t)$ could be modulated by communication messages. In this paper, we do not specify the modulation scheme. The purpose of waveform design in MIMO ISAC thus includes:

- Designing the weights in $\mathbf{W}$, which is more focused on the construction of steering vectors.
- Designing the sequences in $\mathbf{s}(t)$, which emphasizes on the autocorrelation and crosscorrelation.

At the ISAC transceiver, the received echo signal at the i-th receive antenna of the ISAC transceiver is given by

$$\begin{aligned} r_i(t) &= \sum_{n=1}^{N_t}\sum_{k=1}^{K} c_k w_n s_n(t - \tau_{nk} - \tau'_{ki}) \\ &\times \; e^{-j(\omega_c + 2\pi\nu_k)(t-\tau_{nk}-\tau'_{ki})}, \end{aligned} \tag{2}$$

where c_k is the reflection coefficient of target k, τ_{nk} is the traveling time from transmit antenna n to target k, τ'_{ki} is the traveling time from target k to receiver antenna i, and ν_k is the Doppler shift due to the motion of target k, which is given by[1] $\nu_k = \frac{\mathbf{v}_k \cdot \mathbf{q}_k}{\|\mathbf{q}_k\|}\frac{f_c}{c}$. The received signal at the communication antennas is similar to (2), where the delay τ'_{ki} is simply changed to that of communication receive antenna i and c_k is changed to the reflection coefficient in the direction to the communication receiver.

Remark 1 (Difference from Existing MIMO ISAC Modeling): Note that the signal model in (2) is different from the MIMO radar signal model in most standard literature (e.g., Chapter 1 in [5]) where the transmitted signals at different antennas are denoted by complex numbers which imply sinusoidal waveforms. The signal model in (2), more similar to the continuous-time modeling with the fast-time-slow-time structure in Chapter 5 in [5]), considers generic signal waveforms, which is compatible with many non-stationary signals such as FMCW radar waveforms.

2) Discrete-time Signal: For facilitating the waveform analysis, we consider the discrete-time signal obtained from sampling the continuous-time signal s_n with chip period T_c, namely $s_n[l] = s_n(lT_c)$, where the chip period T_c equals the sampling period $\frac{1}{W}$. For simplicity, we assume that T_s is a multiple of T_c and define $N_c = \frac{T_s}{T_c}$.

C. Signal Cube

For the Doppler processing of velocity estimation, we need to consider time duration longer than T_p, due to the necessary accumulation for a significant change of phase. Therefore, we consider L successive pulses, where the antenna index (spatial), intra-pulse time (fast time), and pulse

[1]Here, we omit the difference of directions to different transmit and receive antennas of the ISAC transceiver.

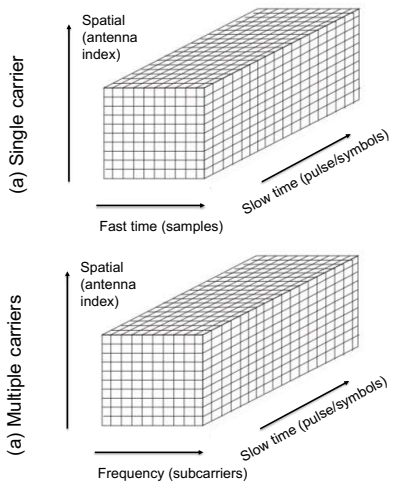

Fig. 2: Signal cube in MIMO ISAC.

index (slow time) for the three dimensions of the signal cube, as illustrated in Fig. 2. We denote the signal cube by $\mathbf{R}_{N_r \times LN_c} = (\mathbf{R}_1, ..., \mathbf{R}_L)$, where $\mathbf{R}_l = (\mathbf{r}_{1l}, ..., \mathbf{r}_{N_r l})^T_{N_r \times N_c}$ is the received signal in the l-th pulse and $\mathbf{r}_{nl}$ is the N_c-dimensional column vector of signals received at the n-th receive antenna in the l-th pulse.

D. Position-Doppler Cells

We also want to discretize the position and Doppler shift for facilitating the sensing procedure. To this end, we consider $Q+1$ possible cells in which the radar target is located. The cells are centered at $\mathbf{q}_0, ..., \mathbf{q}_Q$, where $\mathbf{q}_0$ is the most possible cell (which could be predicted using the history). The Doppler shift is also discretized into $D+1$ possible values $\{\nu_0, \nu_1, ..., \nu_D\}$, where ν_0 is the most probable one. Therefore, we consider $(Q+1)(D+1)$ cells of position-Doppler pairs.

IV. Generalized Ambiguity Function

In this section, we discuss the generalization of AF for the functionality of MIMO ISAC.

A. Traditional Ambiguity Function for SISO

We first introduce the traditional AF in single-input-single-output (SISO) systems. For single-antenna and time-domain signals (thus being scalars), the performance of radar sensing is characterized by the AF proposed by Woodward [6], which is defined as

$$\chi(\tau, \nu) = \int_{-\infty}^{\infty} s(t) s^*(t-\tau) e^{-j2\pi\nu(t-\tau)} dt, \tag{3}$$

where s is the transmitted scalar signal, τ is the time delay and ν is the Doppler-shift. Intuitively speaking, it is desirable to have an AF with a dominant peak at the origin, namely the correltion of received signal and local waveform reaches a dominant peak when the assumed time delay τ and Doppler shift ν match the true values. The sidelobes of AF off the origin may cause confusions in the position or velocity estimation (e.g., marking weak targets). Qualitative requirements on the waveform design are implied from the AF: (a) Positioning: When $\nu = 0$, the AF $\chi(\tau, 0)$ equals the autocorrelation of signal s, which is peaky at $\tau = 0$ when s is similar to a white noise (thus the power spectral density (PSD) is almost constant). (b) Doppler: When $\tau = 0$, the generalized AF $\chi(0, \nu)$ equals the Fourier transform of $|s(t)|^2$, which is peaky at $\nu = 0$ when $|s(t)|^2$ is almost constant. Therefore, in terms of radar sensing performance with scalar signals, it is desirable to have waveforms with constant power and rapid change in the time (e.g., the change of phases), thus large bandwidth with a constant PSD. These features are also shared by good communication signals (less peak-average power ratio (PAPR) and large bandwidth).

B. Generalized Ambiguity Function for MIMO

The traditional AF in (3) is for single-antenna scalar signals. However, for MIMO radar sensing, the signal becomes a vector; therefore it is necessary to revise the definition of AF to characterize the vector signaling.

1) Ranging and Fast Data: In [5] ((3.23) in Chapter 3), a generalized AF is defined for very generic signaling (having MIMO as a special case):

$$A(\theta_0, \theta_1) = E_{p(\mathbf{r}|\theta_0)}[LL(\theta_1|\mathbf{r})], \tag{4}$$

where θ_0 and θ_1 are the hypothesis and true parameters of the target, $\mathbf{r}$ is the received signal, and LL is the log-likelihood. Essentially, the generalized AF is similar to the Kullback-Leibler distance and measures the statistical distance between the parameters θ_0 and θ_1. The generalized AF degenerates to the traditional AF for the single-antenna case. The downsides of this definition include (a) The explicit expression of the generalized AF in (4) is very complicated, even for the simplest Gaussian case (check (3.24) in [5]). (b) The generalized AF in (4) needs detailed probabilistic information, such as the noise probabilistic distribution, which may not be available.

Therefore, we propose a simpler definition for the AF in the spirit of the definition in [5]. Our motivation is that the AF should quantify the similarity between the received signals reflected from the true reflector and a wrong one. Moreover, it is well known that inner product quantifies the similarity between two vectors. Therefore, to this end, we first consider only two position cells and omit the Doppler shift, and define

$$\chi_n(\mathbf{q}_0, \mathbf{q}_1) = \text{trace}\left(\mathbf{R}_n^H(\mathbf{q}_0)\mathbf{R}_n(\mathbf{q}_1)\right), \tag{5}$$

where $\mathbf{R}_n(\mathbf{q})$ is the n-th received signal matrix in the signal cube whose dimensions are fast time and space (antenna index) when the target is at position $\mathbf{q}$, and $\mathbf{q}_0$ and $\mathbf{q}_1$ are the true and hypothesis positions of the radar target (as a

significant reflector). We notice that the definition in (5) is the Frobenius inner product of the matrices $\mathbf{R}_n(\mathbf{q}_0)$ and $\mathbf{R}_n(\mathbf{q}_1)$. The inner product is small when the two matrices are not similar. Therefore, we expect large values of $\chi_n(\mathbf{q}_0, \mathbf{q}_0)$ (which is positive) but small magnitude of $\chi_n(\mathbf{q}_0, \mathbf{q}_1)$ (which could be complex) when $\mathbf{q}_0 \neq \mathbf{q}_1$.

To justify the definition in (5), we can use the Frobenius norm for characterizing the gap between $\mathbf{R}_n(\mathbf{q}_0)$ and $\mathbf{R}_n(\mathbf{q}_1)$ as

$$\begin{aligned} & \|\mathbf{R}_n(\mathbf{q}_0) - \mathbf{R}_n(\mathbf{q}_1)\|_f^2 \\ = \ & \text{trace}\left((\mathbf{R}_n(\mathbf{q}_0) - \mathbf{R}_n(\mathbf{q}_1))^H (\mathbf{R}_n(\mathbf{q}_0) - \mathbf{R}_n(\mathbf{q}_1))\right) \\ = \ & \|\mathbf{R}_n(\mathbf{q}_0)\|_f^2 + \|\mathbf{R}_n(\mathbf{q}_1\|_f^2 \\ - \ & 2\ \text{trace}(\Re(\mathbf{R}_n^H(\mathbf{q}_0)\mathbf{R}_n(\mathbf{q}_1))), \end{aligned} \tag{6}$$

where we apply the fact $\|\mathbf{A}\|_F = \sqrt{\text{trace}(\mathbf{A}^H\mathbf{A})}$ for any complex matrix $\mathbf{A}$.

Therefore, a small value of AF for $\mathbf{q}_0 \neq \mathbf{q}_1$ means large difference between the signal matrices, and thus a better resolution for radar sensing. In contrast to the traditional AF, the AF χ_n plays the role of autocorrelation of the transmitted signal.

2) Doppler Shift and Slow Data: Then, we incorporate the Doppler frequency shift and the L successive pulses (fast-time data matrices). For velocity $\mathbf{v}_0$, the radial speed corresponding to receive antenna k is denoted by v_{0k}, which corresponds to a frequency shift $f_{0k} = \frac{f_c v_{0k}}{c}$ in the received signal at antenna k. Therefore, the received signal in the first fast data matrix is modified to

$$\mathbf{R}_{1,\mathbf{v_0}} = \mathbf{\Theta}_{1,\mathbf{v_0}} \odot \mathbf{R}_1. \tag{7}$$

where $\odot$ is the Hadamard product and the matrix $\mathbf{\Theta}$ characterizing the Doppler shift is given by

$$\mathbf{\Theta}_{1,\mathbf{v_0}} = \begin{pmatrix} 1 & e^{-j2\pi f_{01}T_c} & \dots & e^{-j2\pi(N_c-1)f_{01}T_c} \\ 1 & e^{-j2\pi f_{02}T_c} & \dots & e^{-j2\pi(N_c-1)f_{02}T_c} \\ \vdots & \vdots & \ddots & \vdots \\ 1 & e^{-j2\pi f_{0N_r}T_c} & \dots & e^{-j2\pi(N_c-1)f_{0N_r}T_c} \end{pmatrix}. \tag{8}$$

The operation of Hadamard product makes the decomposition of optimizations of weights $\{w_n\}_{n=1,\dots,N_t}$ and sequences $\{s_n(t)\}_{n=1,\dots,N_t}$ impossible. Fortunately, the phase change within one fast-time data block is small. Therefore, we consider only the phase change due to Doppler shift across different fast data blocks, which is the application of slow-time data in traditional radar systems. Then, the received signal in the n-th block can be approximated by

$$\mathbf{R}_{\mathbf{v_0},n} = \mathbf{\Psi}_{\mathbf{n},\mathbf{v_0}}\mathbf{R}_n, \tag{9}$$

where $\mathbf{\Psi}_{\mathbf{v_0}} = \text{diag}(e^{j2pi\nu_{01}(n-1)T_p}, ..., e^{j2pi\nu_{0N_r}(n-1)T_p})$. Therefore, when the reflector is located at $\mathbf{q}_0$ with velocity $\mathbf{v}_0$, the received signal cube is given by

$$\mathbf{R}(\mathbf{q}_0, \mathbf{v}_0) = (\mathbf{\Psi}_{1,\mathbf{v_0}}\mathbf{R}_1(\mathbf{q}_0), ..., \mathbf{\Psi}_{L,\mathbf{v_0}}\mathbf{R}_L(\mathbf{q}_0)). \tag{10}$$

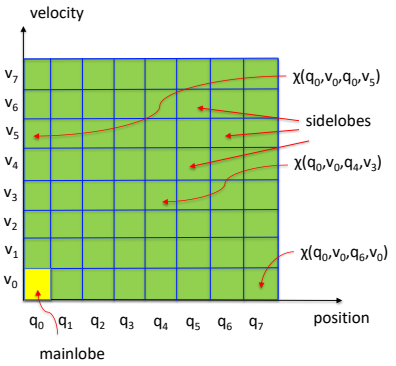

Fig. 3: Mainlobe and slidelobes in the generalized AF.

Similarly to the generalized AF in (5), when the Doppler shift is taken into account, the generalized AF is defined as

$$\chi(\mathbf{q}_0, \mathbf{q}_1; \mathbf{v}_0, \mathbf{v}_1) = \text{trace}(\mathbf{R}^H(\mathbf{q}_0, \mathbf{v}_0)\mathbf{R}(\mathbf{q}_1, \mathbf{v}_1)). \tag{11}$$

3) Multicell and ISL: We expect that the generalized AF to be peaky when $\mathbf{q}_0 = \mathbf{q}_1$ and $\mathbf{v}_0 = \mathbf{v}_1$, which is approximately determined by the transmit power. When $\mathbf{q}_0 \neq \mathbf{q}_1$ and $\mathbf{v}_0 \neq \mathbf{v}_1$, we expect that χ is small, since it implies that the signals received from different positions or velocities be significantly different. In practice, we need to consider many possible cells of range and velocity. Therefore, as illustrated in Fig. 3, the two dimensions of cells form a grid, similarly to the range-Doppler plane for the traditional AF. Suppose that $\mathbf{q}_0$ and $\mathbf{v}_0$ are the correct range and velocity. Therefore, we desire a large mainlobe $\chi(\mathbf{q}_0, \mathbf{v}_0; \mathbf{q}_0, \mathbf{v}_0)$ and small sidelobes $\chi(\mathbf{q}_0, \mathbf{v}_0; \mathbf{q}_q, \mathbf{v}_d)$, where $(q, d) \neq (0, 0)$.

Then, similarly to the definition of integrated sidelobe level (ISL) in traditional AF [6], we define the ISL of MIMO ISAC as the sum of squared magnitudes of sidelobes, namely

$$\xi = \sum_{(q,d)\neq(0,0)} |\chi(\mathbf{q}_0, \mathbf{v}_0; \mathbf{q}_q, \mathbf{v}_d)|^2. \tag{12}$$

V. ISAC Operation and Trade-off

In this section, we discuss the operation in the proposed MIMO ISAC scheme and the corresponding performance trade-off.

A. ISAC Algorithms

We explain the algorithms for sensing and communications, respectively.

1) Sensing: We leverage the AF defined in (5) for sensing. For simplicity, we have an initial guess on the target position $\mathbf{q}_0$ and Doppler shift ν_0 (e.g., obtained from the tracking procedure), while the true position $\mathbf{q}_1$ and true Doppler shift ν_1 are close to $\mathbf{q}_0$. We consider a position-Doppler grid, which is given by

$$\begin{aligned} \Gamma \ = \ & \{(\mathbf{q}_0 + \delta d(m_1, n_1)^T, \nu_0 + \delta v m_2) \\ & \big| m_1, n_1, m_2 = -M, ..., M\}, \end{aligned} \tag{13}$$

where δd and δv are the resolutions of distance and velocity, and Γ forms cells of position and velocity.

For the function of radar sensing in ISAC, we use the following correlation approach, which searches through the cells in Γ and find the one most correlated to the received signal, namely

$$(\mathbf{q}^*, \nu^*) = \max_{\mathbf{q},\nu} \chi(\mathbf{q}_0, \mathbf{q}, \nu), \tag{14}$$

where the signal cube $\mathbf{R}(\mathbf{q}_0)$ is replaced with the received signals.

2) Communications: The communication receiver follows standard matched filter. We assume that the time and frequency have been synchronized at the receiver (e.g., using pilots). Then, the communication symbol x_{nm} in symbol l, without loss of generality, is obtained by

$$x^*_{nm} = \arg\min_x \sum_{l=1}^{N_c} \|x\mathbf{v}^m_{nl} - \mathbf{r}^m_{nl}\|^2, \tag{15}$$

where $\mathbf{v}^m_{nl} = v_{nl}((m-1)T_c : mT_c - 1)$ and $\mathbf{r}^m_{nl} = r_{nl}((m-1)T_c : mT_c - 1)$ are sampled signals. The communication information is embedded in the signal $\mathbf{s}(t)$. In this paper, we consider the communication signaling similarly to code division multiple access (CDMA), namely $s_n(t) = x_{n\lceil \frac{t}{T_s} \rceil} v_n(t)$,

B. Trade-off: Randomness of AF

For simplicity, we consider a single target, namely $K = 1$. Without communications, the waveform synthesis for ISAC degenerates to the traditional MIMO radar one. However, in ISAC, the major challenge is the randomness in the waveforms, namely the transmitted signal $\mathbf{R}_n(t)$ is random due to the modulation of communication symbols. Given the single target assumption, the MIMO AF is given by

$$\chi_n(\mathbf{q}_0, \mathbf{q}_1) = P_t|c|^2 \sum_{m=1}^{N_r} \sum_{n_1,n_2=1}^{N_T} \sum_{m=1}^{T_p} x_{n_1,\lceil \frac{m}{T_s} \rceil} x^*_{n_2,\lceil \frac{m-\delta\tau^m_{n_1.n_2}}{T_s} \rceil} v_{n_1}[m] v^*_{n_2}[m - \delta\tau^m_{n_1.n_2}], \tag{16}$$

where $\delta\tau^m_{n_1,n_2}$ is the delay difference of the signals from transmit antennas n_1 and n_2 to receive antenna m, when the target positions are $\mathbf{q}_0$ and $\mathbf{q}_1$, respectively.

Because of the randomness in the communication symbols $\{x_{n,m}\}_{n,m}$, the value of AF also becomes random. Therefore, we need to consider the expectation of χ_n. Notice that the data packets along different antennas are mutually independent; thus the expectations of the cross-correlations of signals sent from different transmit antennas are nullified. Therefore, the expectation of the AF (without Doppler shift) is given by

$$\begin{aligned} E[\chi_n(\mathbf{q}_0, \mathbf{q}_1)] &= P_t|c|^2 \sum_{m=1}^{N_r} \sum_{n=1}^{N_T} \sum_{m=1}^{T_p} v_n[m] v^*_n[m - \delta\tau^m_n] \\ &\times I(|\delta\tau^m_n| < N_c), \end{aligned} \tag{17}$$

where $I(|\delta\tau^m_n| < N_c)$ is the indicator function which equals 0 when the delay difference $\delta\tau^m_n$ is greater than N_c such that

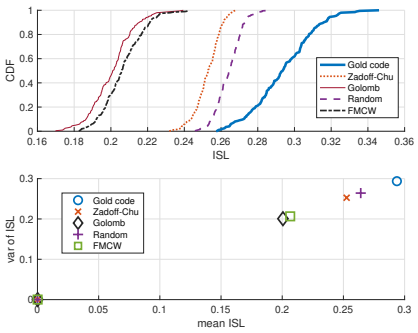

Fig. 4: ISL CDF, expectation and variance of Raning.

the communication symbols $x_{n,\lceil \frac{m}{T_s} \rceil}$ and $x^*_{n,\lceil \frac{m-\delta\tau^m_n}{T_s} \rceil}$ have different indices and thus become uncorrelated.

The results in (17) could be misleading, since it seems that the randomness of communication data reduces the ISL, due to the extra term $I(|\delta\tau^m_n| < N_c)$ in (17). To fairly assess the performance, we need to take the variance of the AF into account as well. With some algebra omitted due to the limited space, we obtain

$$Var[\chi_n(\mathbf{q}_0, \mathbf{q}_1)] = E[\chi^2_n(\mathbf{q}_0, \mathbf{q}_1)] - E^2[\chi_n(\mathbf{q}_0, \mathbf{q}_1)], \tag{18}$$

where

$$\begin{aligned} E[\chi^2_n(\mathbf{q}_0, \mathbf{q}_1)] &= P_t^2|c|^2 \sum_{n_1,n_2=1}^{N_t} \sum_{m_1=1}^{N_cN} \sum_{m_2 \sim m_1} \\ & v_{n_1,m_1} v^*_{n_1,m_1-\delta\tau^{m_1}_{n_1,n_2}} v^*_{n_2,m_2} v_{n_2,m_2-\delta\tau^{m_2}_{n_1,n_2}} \\ &+ \xi(n_1, n_2, m_1, \delta\tau). \end{aligned} \tag{19}$$

and $m_1 \sim m_2$ means $\left\lceil \frac{m_1}{N_c} \right\rceil = \left\lceil \frac{m_2}{N_c} \right\rceil$, namely the corresponding communication symbols are the same, and the correction term ξ is given by $\xi(n_1, n_2, m_1, \delta\tau) = I(n_1 = n_2, m_1 \sim m_1 - \tau)\left(E[|x|^4] - P^2\right)$.

For the waveform synthesis, our goal is to minimize the ISL in (12). Since the ISL in (12) is a random variable, we consider the expectation of ISL. Meanwhile, the variance of ISL also needs to be controlled. To this end, we have

$$E[ISL] = Q \sum_k \sum_l E\left[\left|\chi_n(\mathbf{q}_0, \mathbf{q}_k, \nu^l)\right|^2\right], \tag{20}$$

whose proof is omitted.

VI. Numerical Results

In the numerical simulations, we consider the 28GHz band and assume a 2GHz bandwidth. The code length is 1024, while pulse duration is $L = 64$ (namely 30us). For the ISAC transceiver, we assume 16 transmit antennas, while 16 receive antennas are co-located with them. We consider the schemes of gold code, Zadoff-Chu code, Golomb code, random code and FMCW.

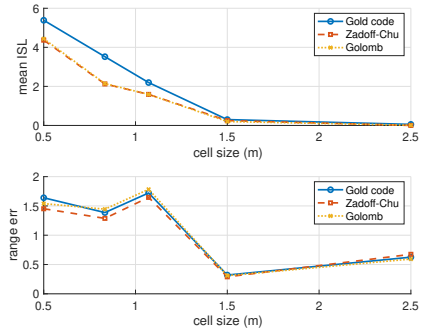

Fig. 5: Sensing error versus cell size.

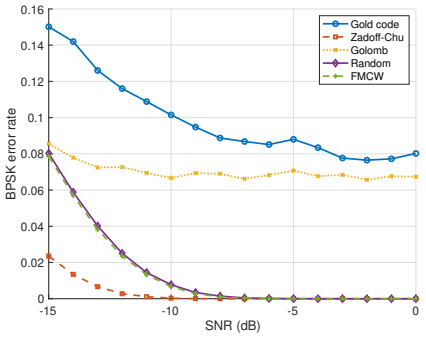

Fig. 6: Bit error rate in communications.

Figure 4 shows the cumulative distribution functions (CDFs), expectations and variances of the five coding schemes, for ranging when assuming no Doppler shift. We observe that the Golomb code achieves both the minimum expectation and variance of ISL, while FMCW has a very close performance.

Figure 5 shows the expected ISL and average sensing error as functions of the cell size for three coding schemes. We observe that, again, the Golomb code achieves the best performance. Although the expected ISL decreases monotonically with the cell size, the sensing error does not, since a coarse cell definition incurs inherent quantization errors.

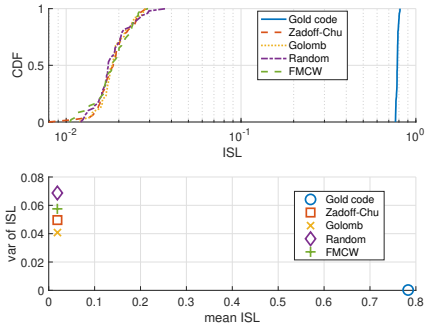

Fig. 7: ISL CDF, expectation and variance of Doppler.

Figure 7 shows the ISL CDF, expectation and variance (normalized by the square mean) of Doppler for speed between 0 and 40 meters, using 64 pulses. We observe that, except for the Gold code, all other codes achieve very similar performances. Moreover, the variances are very small, which implies negligible impact of communications on the Doppler velocity estimation.

VII. Conclusions

In this paper, we have discussed the ISAC waveform design for MIMO transceivers, in which all dimensions of time, frequency and space are taken into account. We have defined a generalized AF for the MIMO case. Numerical simulations have been carried out to compare the waveforms based on different codes.

References

[1] H. Li, "Dirty paper coding for waveform synthesis in integrated sensing and communications: A broadcast channel approach," in *IEEE International Conference on Communications (iCC)*, 2022.

[2] ——, "Performance trade-off in inseparable joint communications and sensing: A pareto analysis," in *IEEE International Conference on Communications (ICC)*, 2022.

[3] ——, "Functional multiplexing with waveform diversity in joint communications and sensing: A superposition coding framework," in *submitted to 3rd IEEE International Symposium on Joint Communications & Sensing*, 2023.

[4] R. W. H. Jr and A. Lozano, *Foundations of MIMO Communications*. Cambridge University Press, 2019.

[5] J. Li and P. Stoica, *MIMO Radar Signal Processing*. Wiley, 2009.

[6] J. L. H. He and P. Stoica, *Waveform Design for Active Sensing Systems: A Computational Approach*. Cambridge University Press, 2012.

[7] L. Zheng, M. Lops, Y. C. Eldar, and X. Wang, "Radar and communication co-existence: An overview," *arXiv preprint arXiv:1902.08676*, 2019.

[8] F. Liu, C. Masouros, A. Petropulu, H. Griffiths, and L. Hanzo, "Joint radar and communication design: Applications, state-of-the-art, and the road ahead," *IEEE Transactions on Communications*, 2020.

[9] D. Ma, N. Shlezinger, T. Huang, Y. Liu, and Y. C. Eldar, "Joint radar-communications strategies for autonomous vehicles," *IEEE Signal Processing Magazine*, vol. 37, no. 4, pp. 85–97, 2020.

[10] B. Paul, A. R. Chiriyath, and D. W. Bliss, "Survey of rf communications and sensing convergence research," *IEEE Access*, vol. 5, pp. 252–270, 2016.

[11] A. Goldsmith, S. A. Jafar, N. Jindal, and S. Vishwanath, "Capacity limits of MIMO channels," *IEEE Journal on Selected Areas in Communications*, vol. 21, no. 5, pp. 684–702, 2003.

[12] Y. Ma, Z. Yuan, G. Yu, S. Xia, and L. Hu, "A spectrum efficient waveform integrating OFDM and FMCW for joint communications and sensing," *Proc. of IEEE ICC 2022 Workshop on Integrated Sensing and Communications*, 2022.

[13] H. Ju, Y. Long, X. Fang, Y. Fang, and R. He, "Adaptive scheduling for joint communication and radar detection: Tradeoff among throughput, delay and detection performance," *IEEE Trans. on Vehicular Technology*, vol. 71, no. 1, pp. 670–680, 2022.

[14] P. Kumari, S. A. Vorobyov, and R. W. H. Jr, "Adaptive virtual waveform design for millimeter-wave joint communication-radar," *IEEE Trans. on Signal Processing*, vol. 68, no. 6, pp. 715–729, 2022.

[15] C. Meng, Z. Wei, and Z. Feng, "Adaptive waveform optimization for mimo integrated sensing and communication systems based on mutual information," in *The 14th International Conference on Wireless Communications and Signal Processing (WCSP)*, 2022.

[16] Z. Gao, Z. Wan, D. Zheng, S. Tan, C. Masouros, D. W. Kwan, and S. Chen, "Integrated sensing and communication with mmwave massive mimo: A compressed sampling perspective," *IEEE Trans. on Wireless Communications*, vol. 22, no. 3, pp. 1745–1762, 2023.